The Investigation of Alkali Silica Reaction of Mortars Containing Borogypsum

Kursat Yildiz(✉)

Technology Faculty, Civil Engineering Department, Gazi University, Ankara, Turkey
kursaty@gazi.edu.tr

Abstract. In this study, various properties and the alkali silica reaction (ASR) of mortars containing borogypsum were investigated. In the first stage a complete physical, chemical, mineralogical, molecular characterization of the borogypsum and cement were performed. In the second stage, the alkali silica reaction, mechanical and porosity properties of mortars, replacement 0, 1, 2, 3 and 4% borogypsum by weight were determined. According to experimental result, from a mineralogical perspective, the borogypsum was observed to have a sharp crystal structure and possess a mineralogical composition of calcite, colemanite and celestine. Looking from a molecular perspective, the similar OH, CaO, B–OH and H–OH bonds were displayed in the close wavenumbers. As the results of 14 days measurements were analyzed, the average maximum length extension was detected to be in the control mortar bars and at the detrimental zone from the ASR perspective. The average minimum length extension at the borogypsum with a additive rate of 3 and 4%, was observed to be at the control zone from ASR perspective. The lowest strength loss in mortars exposed to ASR effect occured in those with substitution level of 3% borogypsum. When the flexural strength of mortars exposed to ASR effect was examined, the increase in strength was observed for borogypsum with all substitution levels (1–4%). The maximum recovery concerning the minimum volume of mercury intruding the sample and vacancy rate was observed for the substitution level 3% borogypsum.

Keywords: Porogypsum · Alkali silica reaction
Mineralogical-mechanical property · Porosimetry

1 Introduction

Its use as aggregate in materials may in certain circumstances lead to alkali silica reaction (ASR) related problems. ASR is one of the most studied deleterious degradation mechanisms of concrete, which is particularly harmful. Once detected in a concrete structure, ASR is very difficult to stop. It is nowadays possible to use mineral additions like natural pozzolans or sub-products with pozzolanic reactivity to inhibit ASR in new concrete [1].

Alkali silica reaction (ASR) is one of the degradation process and refers to chemical reaction between the reactive silica phases in the aggregates and the alkali hydroxides

S. Fırat et al. (eds.), *Proceedings of 3rd International Sustainable Buildings Symposium (ISBS 2017)*, Lecture Notes in Civil Engineering 7,
https://doi.org/10.1007/978-3-319-64349-6_30

in the pore solution of cement-based materials. The reaction results in the formation of alkali–silica gels and/or alkali–calcium–silica gels. These gels which absorb water and swell can lead to the formation of micro cracks [2–10].

Adjustments and improvements to the present concrete making methods are essential in order to address environmental and economic issues. This has encouraged researchers in the area of concrete engineering and technology to investigate and identify supplementary by-product materials that can be used as substitutes for constituent materials in concrete production [11]. Borogypsum is formed by reacting colemanite with sulphuric acid in the production of boric acid and is obtained by filtering the reaction mixture on the filter presses. The material mainly consists of gypsum, B_2O_3 and some impurities and causes various environmental and storage problems. B_2O_3 is dissolved by rain water and mixed with soil. High amount of boron content, which has toxicological effect, leads economic losses and also causes environmental pollution [12–14].

Boron is one of the most important ores in Turkey which possesses 72% of the world boron reserves. The most important boron minerals in Turkey are colemanite, ulexite and tinkal. The amount of Borogypsum waste is approximately 550,000 tons per year. Therefore, its positive effects on concrete properties borogypsum have recently been drawn attention by some researchers [15].

There are a number of studies in the literature which investigated the use of borogypsum as a cement additive [15–18].

Some studies focused on the use of borogypsum in mortar production as a cement replacement [19–22]. On the other hand, some researchers studied leaching kinetics of borogypsum by leaching with water [20–25]. However, only a few studies investigated the effect of borogypsum on the properties of concrete specimens [26, 27]. It is believed that has an effect borogypsum on the strength and consistency properties of concrete warrants further research.

There are a number of studies in the literature which investigated the use of pore size distributions which were measured using mercury intrusion porosimetry (MIP). Mercury intrusion porosimetry (MIP) is a widely used technique for characterizing the distribution of pore sizes in cement-based materials. It is a simple and quick indirect technique, but it has limitations when applied to materials that have irregular pore geometry [28–31].

The primary objective of this study is to investigate the usability of borogypsum in cementbased mortars a mineral additive and its effect on XRD analysis, FT-IR analysis, expansion test, compressive and flexural strength and mercury intrusion porosimetry (MIP) tests.

2 Materials and Methods

In this study, standard Portland Cement CEM I (PC 42.5 N/mm^2) with a specific gravity of 3.17 g/cm^3 was used. Initial and final setting times of the cement were 160 and 210 min, respectively. The blaine specific surface area was 3625 cm^2/g. Borogypsum used in the experiments was supplied by Etibor Bandırma Borax and Boric Acid Plants in Turkey. The specific gravity of Borogypsum was 2.25 g/cm^3.

Blaine specific surface area was 19170 cm^2/g. The remaining of the borogypsum on 50 and 20% sieves were 5 and 1.3 μm respectively. Elemental analyses of samples were carried out by X-ray fluorescence (XRF) spectrometry technique. Chemical, physical, XRD, FT-IR and Porosimetry analyses were conducted for the samples used in the experiments. Chemical analyses of cement and borogypsum are performed on ARL 8680 S X-ray diffraction. Surface areas are determined as Blaine values by Toni Technic 6565 Blaine and specific weights are determined by Quantachrome MVP-3. The mineralogical properties are determined by Rikagu miniflex XRD device using Cu K_α (λ = 1.54 Å) radiation. FT-IR analyses are conducted using Bruker Vertex 70 in the wave number range of 400–4000 cm^{-1}. Pore size distributions were measured using mercury intrusion porosimetry (MIP) [32].

The chemical compositions of cement and borogypsum are presented in Table 1. The grain distribution of borogypsum is shown in (Fig. 1).

Table 1. Chemical composition of cement and borogypsum

Materials	Cement	Borogypsum
Chemical composition: wt%		
SiO_2	20.01	4.55
Al_2O_3	5.15	1.30
Fe_2O_3	3.51	0.35
CaO	62.97	27.72
MgO	2.25	1.48
SO_3	2.95	37.75
Na_2O	0.47	–
K_2O	0.87	0.77
B_2O_3	–	4.30
Loss on ignition	2.17	21.78
CaO free	–	–

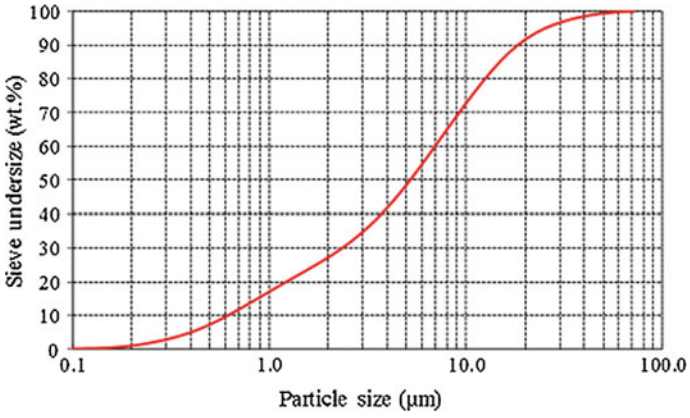

Fig. 1. The grain distribution of borogypsum

Dry and clean natural crushed stone aggregates were used with a maximum size of 4 mm. The absorption value and relative density at saturated (A-RD-SSD) condition of aggregate were WA_{24} = 1.2% and ρ_a = 2.71, ρ_{rd} = 2.65, ρ_{ssd} = 2.66 respectively. The methylene blue value of aggregate was M_B = 0.75 g/kg. Other characteristics of the aggregates are provided in Table 2. The compositions of each aggregate group are illustrated in Table 3. City water of the province of Ankara was used.

Table 2. The characteristics of the aggregates

Characteristics	Standards	Results
Very fine material	TS EN 933-1	%9
Bulk density (mg/m^3)	TS EN 1097-3	1.65
Chlorides (%)	TS EN 1744-1	0.0042
Acid-soluble sulfate (%)	TS EN 1744-1	AS0.2 $\leq$ 0.2
Total Sulfur (%)	TS EN 1744-1	0.009
Organic matter	TS EN 1744-1:15.1	–
Fulvo acid content	TS EN 1744-1:15.2	–
Lightweight organic pollutants	TS EN 1744-1:14.2	MLPC = 0.0%

Table 3. Aggregate gradation

Sieve size	The remaining material between of the two sieve (%)
4.75 mm (no: 4)–2.36 mm (no: 8)	10
2.36 mm (no: 8)–1.18 mm (no: 16)	25
1.18 mm (no: 16)–600 μm (no: 30)	25
600 μm (no: 30)–300 μm (no: 50)	25
300 μm (no: 50)–150 μm (no: 100)	15

In this study, the cement was used for the preparation of reference samples. Borogypsum was blended in this cement at rates of 0, 1, 2, 3 and 4%. Therefore, a total of five different cements were used and those were codified as (Boron Gypsum-BG) BG0, BG1, BJ2, BG3 and BG4. The compositions of each mortar sample (25 × 25 × 285 mm^3) mixture are illustrated in Table 4. Mortar bar were prepared according to the

Table 4. Mortar samples mixture ratio for ASR (g)

Mixture	Borogypsum	Cement	Aggregate	Water	W/C
BG0	0	440	990	206.8	0.47
BG1	4.4	435.6	990	206.8	
BG2	8.8	431.2	990	206.8	
BG3	13.2	426.8	990	206.8	
BG4	17.6	422.4	990	206.8	

ASTM C 1260-07 standard [33]. They were demoulded 24 h after casting, and after were immersed in water at 23 °C and stored in a climatic chamber at 80 °C for 24 h. After this period, the initial length of each prism was measured (zero point or initial point), after which the prisms were immersed in a NaOH 1 M solution at 80 °C for 14 days. During this period of time, regular length measurements were taken at various ages to check the progress of the expansion. According to the test limits a mix that has an expansion at 2, 7 and 14 days below 0.10% are considered non-reactive (harmless zone) and are considered reactive (harmful zone) if that expansion is higher than 0.20%.

The prepared mortar samples were poured into the ($40 \times 40 \times 160$ mm^3) prismatic formworks for flexural and compressive strength tests. The compositions of each mortar sample mixture are illustrated in Table 5 [34]. These mortar specimens were shaken for one minute on a shaking table then settled into the formworks. These specimens were kept in a laboratory environment for 24 h. At the end of this duration, the specimens were taken out of the formworks and kept in the half ASR cure other half water curing pool. The specimens were taken from the water and ASR pool after 28 day and were tested for flexural and compressive strengths in accordance with [35].

Table 5. Mortar samples mixture ratio for flexural and compressive strength tests

Mixture	Borogypsum	Cement	Aggregate	Water	W/C
BG0	0	660	1485	310.2	0.47
BG1	6.6	653.4	1485	310.2	
BG2	13.2	646.8	1485	310.2	
BG3	19.8	640.2	1485	310.2	
BG4	26.4	633.6	1485	310.2	

3 Experimental Results and Discussion

3.1 Chemical Analysis

According to the chemical analysis results, cement consists of CaO and SiO_2 with higher proportion and Al_2O_3, Fe_2O_3 and SO_3 compounds with lower proportion. The main component of borogypsum is SO_3 and CaO the ratio of SiO_2/Al_2O_3 (S/A) is 3.50 in weight. The total of $SiO_2 + Al_2O_3 + Fe_2O_3$ is 6.20 in weight. To be accepted as a mineral pozzolan S/A > 4 and $SiO_2 + Al_2O_3 + Fe_2O_3 > 70$ should be. Therefore, the use of borogypsum is not true as a pozzolan [36].

3.2 Mineralogical Analysis

XRD analyses are conducted to determine the mineralogical structure of cement and zeolite (Figs. 2 and 3). According to the XRD patterns, the main components of cement

CEM I (PC 42.5 N/mm^2) are [C_3S-Alite ($3CaOSiO_3$), C_2S-Belit ($2CaOSiO_3$), Cc-Calcite ($CaCO_3$), CH-Portlandite ($Ca(OH)_2$) and brownmillerite ($Ca_2(Al,Fe_2^{3+})O_5$]. The XRD results indicate that the structure of cement is regular (crystal) (Fig. 2) Borogypsum consists of [Calcite –($CaCO_3$), Colemanite-($Ca_2B_6O_{11}\cdot 5H_2O$), Celestine-($SrSO_4$)]. The XRD results indicate that the structure of borogypsum is sharp (crystal) (Fig. 3) [37].

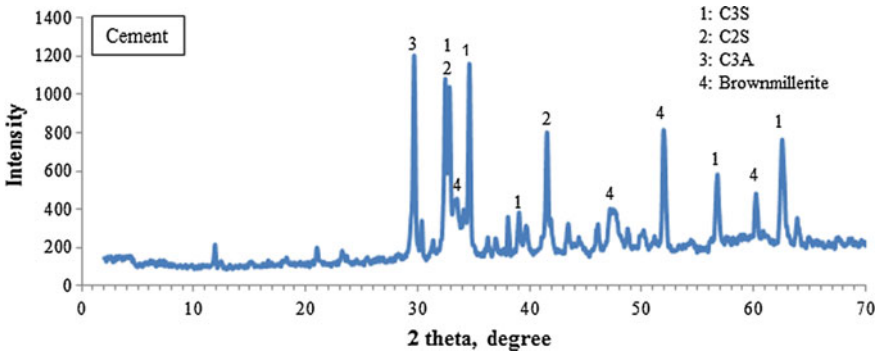

Fig. 2. The mineralogical structure of cement

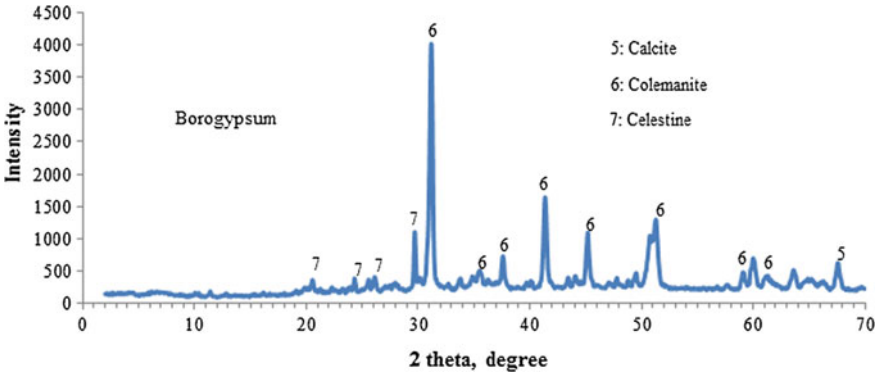

Fig. 3. The mineralogical structure of borogypsum

3.3 FT-IR Analysis

FT-IR analyses are available to characterize molecule groups in a particle. In the FT-IR studies are related to cement and pozzolan, the infrared spectrum to be regarded as in

mainly 4 wide band regions. They are consisting of peaks corresponding to the deviations in Si–Al, S, C and OH bonds [38]. Surface structures of the molecules are determined from the FT-IR results indicated from the analyses and shown in (Figs. 4 and 5) in the manner of a schematic.

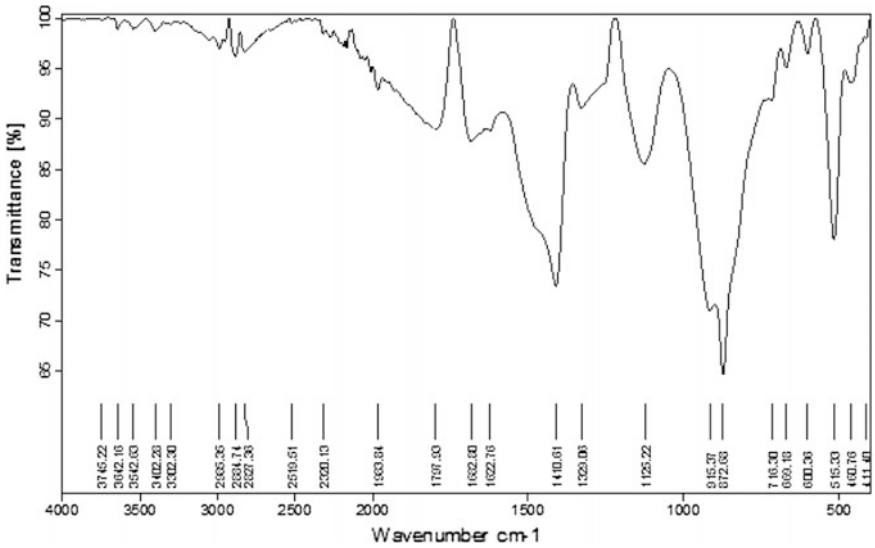

Fig. 4. FT-IR spectrum of cement

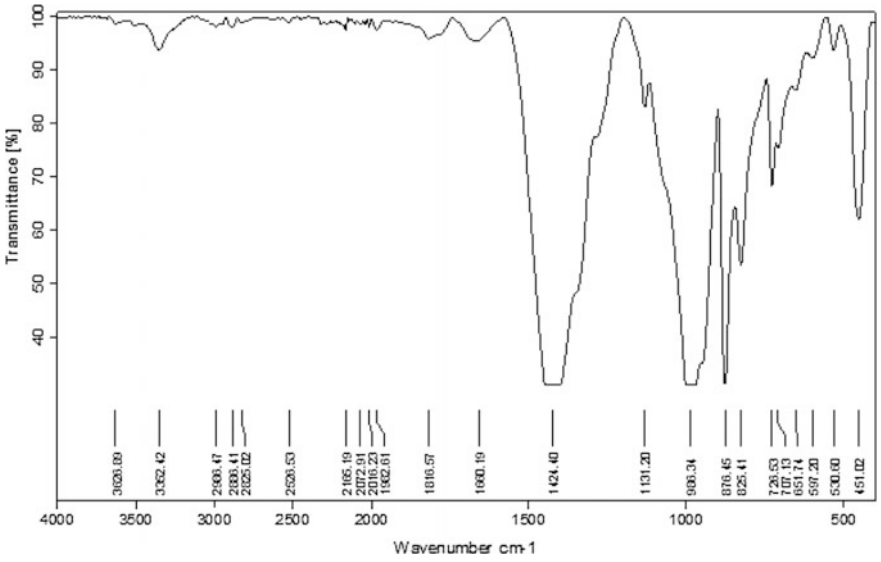

Fig. 5. FT-IR spectrum of borogypsum

In FT-IR spectroscopy, vibration of the atoms forming solid cages and molecular vibrations are observed in 400–1600 and 1600–4000 cm^{-1} region, respectively. Vibration peaks are displayed at 461, 516, 601, 669, 873, 915, 1125, 1410, 3402 and 3642 cm^{-1} wave numbers from FT-IR analysis of cement (Fig. 4). Si–O bonds present with Al–O give vibration peaks of 461 and 516 cm^{-1}. Si–O bonds in cage structures are in the form of a vibration peak at 872 cm^{-1} wave number. S–O bonds which show the plaster in cement is seen at 601, 1125 and 1623 cm^{-1}. Vibration peak of water ions and molecules in the structure is at 3302 and 3642 cm^{-1} wave number [39, 40].

FT-IR spectra can obtain advantageous information on borogypsum mineral structure. The spectrum of borogypsum over the 500–4000 cm^{-1} spectral range is displayed in (Fig. 5). Vibration peaks are displayed at 451, 597, 727, 825, 876, 986, 1424, 1660, 1816, 3352 and 3627 cm^{-1} wave numbers from FT-IR analysis of borogypsum. The absorptions at 1660, 1816, 3626 and 3352 cm^{-1} are due to intermolecular and weakly H bonded OH because of water of crystallizations [41]. CaO vibrations are observed in 451 cm^{-1} region. The spectrum of borogypsum is dominated by a strongest vibration band at 986 cm^{-1}. This peak is attributed to the bending mode in the shape of trigonal symmetric vibration. Symmetric vibration peak at 876 cm^{-1} wave number tetrahedral the presence of boron in the structure, a strong peak at 1424 cm^{-1} wave number in the trigonal structure indicates the presence of boron. The vibration peaks at 727 and 825 cm^{-1} may be assigned to the out-of-plane B-OH bending modes [42].

3.4 Expansion Results

CEM I and borogypsum were determined of equivalent alkaline value as (1.04) and (0.50) respectively. These values were calculated with equation of state (Na_2O + $0.658K_2O$). Figure 6 shows the evolution of the average expansion of (BG1, BG2, BG3 and BG4) mortar and (BG0) mortar.

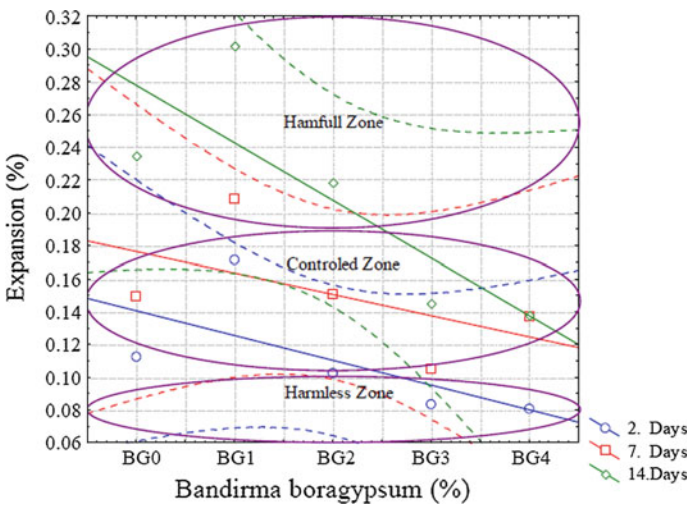

Fig. 6. The expansion of borogypsum

When the longitudinal elongation values depending on time were evaluated in 2, 7 and 14 days of periods;

At the end of 2 days measurements, while the control mortar bar with no borogypsum replacement took part in BG0 controlled zone (harmful-harmless zone) BG1 mortar bar with 1% borogypsum replacement (although staying in the controlled zone) exhibited maximum value in the 2 days group. This situation, depending on the increase of borogypsum replacement, stayed at limit values in BG2, stayed at the harmless zone in BG3 and BG4 mortar bars from the point of longitudinal elongation. When generally taking a look at at the 2 days measurement group, it is thought that the usage of 2, 3 and 4% replacement ratios will provide positive results in the first years of service period of cement mortars from the point of ASR.

At the end of 7 days measurements, while the control mortar bar with no borogypsum replacement took part in BG0 controlled zone (harmful-harmless zone) BG1 mortar bar with 1% borogypsum replacement stayed in the harmful zone and exhibited a maximum longitudinal elongation value in the 7 days group. Depending on the increase of borogypsum replacement ratio BG2 and BG4 took part in the controlled zone. BG3 exhibited optimal value in the 7 days measurement group and took a 0.105% value which is very close to the harmless zone. When taking a look at the 7 days measurement group, as in the 2 days measurement group, it is thought that the usage of 2, 3 and 4% replacement ratios will provide positive results from the point of ASR at the middle ages of the service life of cement mortars and the usage of 3% borogypsum will exhibit optimal result.

At the end of 14 days measurements, it was observed that the control mortar bar BG0 with no borogypsum replacement took part in the harmful zone from the point of ASR. Depending on the increase of borogypsum replacement ratio, the harmful zone could not be overcome at the BG1, BG2 and BG3 mortar samples. During the service life of cement mortars, it was observed from the point of ASR that 4% borogypsum replacement could be used for all of the three age group.

3.5 Flexural and Compressive Strengths of Bandirma Borogypsum Replacement Mortars Under the Effect of Alkali–Silica Reaction

For the purpose of determining the mechanical strength loss in the mortars due to ASR effect, flexural and compressive tests were applied to the control species kept in the water curing pool for 28 days and to the mortars subjected to ASR effect. The experimental data was evaluated at the 95% confidence band among each other in each group containing three species in different replacement ratios and was observed to be statistically reasonable. The scatter plots belonging to this statistical analysis are given in Figs. 7 and 8.

From the point of Compressive Strength;

When the mortars with Bandırma borogypsum replacement (not subjected to ASR effect) were evaluated among each other, BG0 control mortar sample with no borogypsum replacement exhibited maximum compressive strength. Depending on the increase of replacement ratio, BG1 and BG3 mortars samples and BG2 and BG4 samples exhibited similar behavior from the point of compressive strength. When these

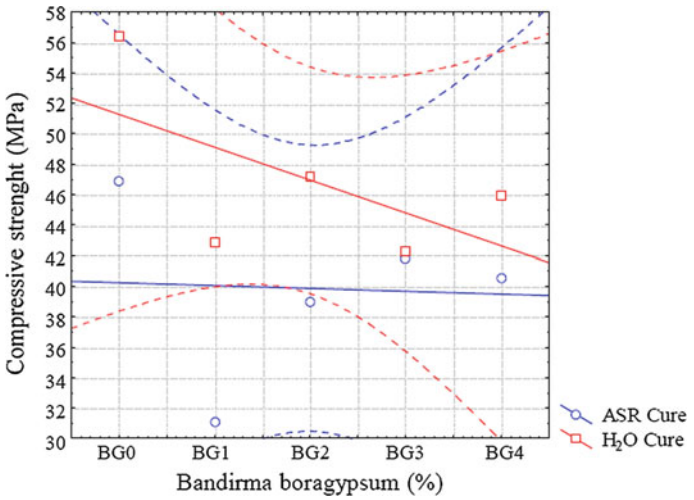

Fig. 7. The compressive strength of borogypsum

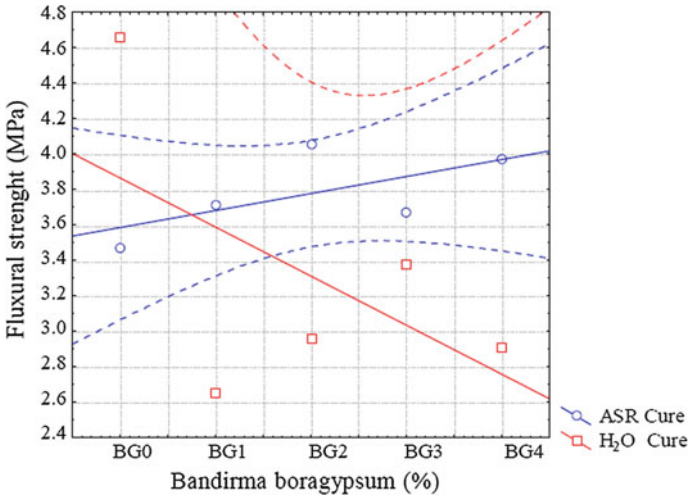

Fig. 8. The flexural strength of borogypsum

groups were considered, BG2 and BG4 mortars groups showed higher compressive strength compared to BG1 and BG3 mortars groups. When the samples with no ASR effect were evaluated, it was observed that increase of borogypsum replacement caused compressive strength loss.

When the mortars with borogypsum replacement (subjected to ASR effect) were examined among each other, control mortar sample exhibited maximum compressive strength, whereas BG1 mortar sample showed minimum compressive strength. While the

BG2 and BG4 samples were exhibiting values close to each other, maximum compressive strength in the group with replacement was observed in the BG3 mortar sample.

When the samples with ASR effect and with no ASR effect were compared with each other, compressive strength loss was observed in all of the samples under ASR effect. This loss occurred at an acceptable level in BG3 mortar group.

From the point of Flexural Strength;

When the mortar samples having no ASR effect were examined, a flexural loss was observed in all of the replacement ratios compared to control group BJ0 mortar samples at different levels. This loss occurred in BG1, BG2, BG4 and BG3 mortar groups from the highest to the lowest respectively.

When the mortar samples (subjected to ASR effect) were examined, no flexural loss was observed in all of the replacement ratios compared to BG0 mortar samples. On the contrary an increase in the flexural strength was seen in BG2, BG4, BG1 and BG3 mortar groups from the highest to the lowest respectively.

When the samples which were subjected and not subjected to ASR effect were compared with each other a serious flexural loss was observed in the control mortar group with no replacement, whereas in the other, replacement ratios at different levels a flexural strength increase was observed. Like in the compressive strength, the closest flexural strength was observed in the BG3 replacement ratio.

3.6 Porosity Volumes of Mortars with Bandırma Borogypsum Replacement

The relationship between the porosity diameter belonging to Bandırma borogypsum and mercury volume (intruding cumulatively) is given in in the graphs of Fig. 9. From the graphic, it is seen that the cumulative mercury volume intruding to samples is observed in the control group BG0 mortar sample in the highest amount. Whereas in all

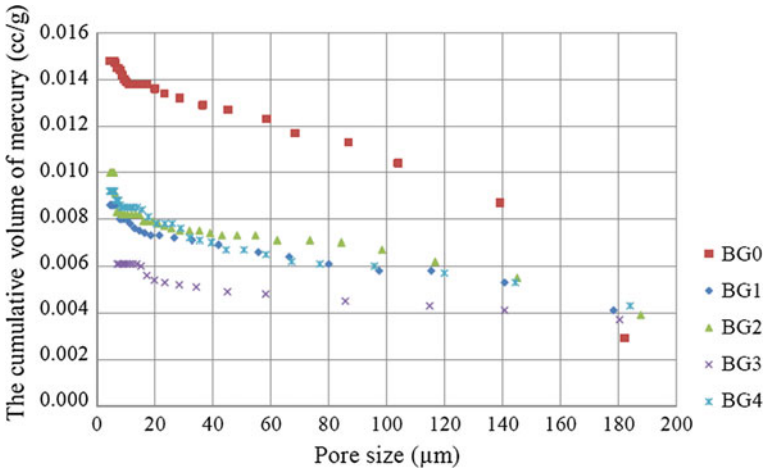

Fig. 9. Pore size distribution of mortars

of the replacement ratios less mercury intrusion was realized compared to control group. This can be accepted as an indication of Bandırma borogypsum mortar samples reducing the porosity volume in various portions. Because mortar samples exhibited different porosities at various borogypsum ratios. This occurred in the BG2, BG4, BG1 and BG3 mortar groups from the highest to the lowest respectively. BG2, BG4 and BG1 mortar samples exhibited very close values from the point of cumulative intruding mercury volume. Whereas BG3 provided a maximum improvement from the aspect of porosity ratio with minimum mercury intrusion.

4 Conclusions and Suggestions

Longitudinal elongation, compressive strength and flexural strength tests were carried on for the determination of alkali silica reaction behavior of borogypsum in mortars. Besides, mineralogical and molecular analyses of the used materials were made. Furthermore, the effect of borogypsum containing mortars on the porosity ratio was analyzed.

From the point of mineralogical and molecular structure;

- When the XRD analysis result of borogypsum was examined, it was observed that it was formed by [Calcite–($CaCO_3$), Colemanite–($Ca_2B_6O_{11}{\cdot}5H_2O$), Celestine ($SrSO_4$)]. It was a sharp crystal from the point of general structural view.
- From the molecular point, it exhibited –OH, B–O and B–OH bonds.

From the aspect of ASR;

- When a general look was taken at the 2 days measurement group it was observed that the 2, 3 and 4% usage of replacement ratios could provide positive results in the first years of cement mortar service life from the point of ASR.
- When the 7 days measurement group was considered, as in the 2 days measurement group, the 2, 3 and 4% usage of replacement ratios could provide positive results in the middle ages of cement mortar service life from the point of ASR and 3% usage of borogypsum could exhibit optimal results.
- During the service life of cement mortars, from the point of ASR, it was observed that 4% borogypsum replacement could be used in all of the three age groups.

The optimal replacement amount for ASR must be determined not only according to the length elongation but also be made by considering the mechanical strengths. From the point of mechanical properties;

- When the samples that were not subjected to the effect of ASR were evaluated, it was observed that the increase in the borogypsum replacement caused compressive strength loss.
- When the samples that were subjected and not subjected to ASR effect were compared with each other, a compressive strength loss was observed in all of the samples subjected to ASR effect. This loss was at an acceptable level in the BG3 mortar group.

- When the samples that were subjected and not subjected to ASR effect were compared with each other a serious flexural loss was observed in the control mortar group with no replacement whereas in all of the other replacement ratios an increase in the flexural strength was observed at various levels. As in the compressive strength the closest flexural strength was determined with the BG3 replacement ratio.

From the point of porosity volume;

- The cumulative mercury volume intruding to samples was observed in the control group BJ0 mortar sample in the highest amount.
- Mortar samples exhibited different porosities at various borogypsum ratios. This situation occurred in the BG2, BG4, BG1 and BG3 mortar groups from the highest to the lowest respectively.
- Whereas in the BG3 replacement ratio, maximum improvement was obtained from the point of porosity ratio with minimum mercury intrusion.

Acknowledgements. This study was supported by Gazi University Scientific Researches Project Department with 07/2012-03 project code number. I thank to my university and to the valuable members for their supports.

References

1. Serpa D, Santos Silva A, de Brito J, Pontes J, Soares D (2013) ASR of mortars containing glass. Constr Build Mater 47:489–495
2. Neville AM (1995) Properties of concrete, 4th edn. Longman Group, Harlow
3. Carles-Gibergues A, Hornain H (2008) La durabilité des bétons face aux réactions de gonflement endogène. In: Ollivier JP, Vichot A (eds) La durabilité des bétons: bases scientifiques pour la formulation de bétons durables dans leur environnement. Presses de l'Ecole Nationale des Pons et Chaussées, Paris, pp 487–611 (in French)
4. Fournier B, Bérubé MA, Thomas MDA, Smaoui N, Folliard KJ (2004) Evaluation and management of concrete structures affected by alkali–silica reaction—a review. MTL 2004–2011 (OP), Natural Resources Canada, Ottawa
5. Godart B, Le Roux A (1995) Alcali-réaction dans le béton: mécanisme, pathologie et prévention. Techniques de l'Ingénieur, traité de Construction, C 2 252 (in French)
6. Marzouk H, Langdon S (2003) The effect of alkali-aggregate reactivity on the mechanical properties of high and normal strength concrete. Cem Concr Compos 25:549–556
7. Poyet S, Sellier A, Capra B, Foray G, Torrenti JM, Cognon H et al (2007) Chemical modelling of alkali silica reaction: influence of the reactive aggregate size distribution. Mater Struct 40:229–239
8. Garcia-Diaz E, Riche J, Bulteel D, Vernet C (2006) Mechanism of damage for the alkalisilica reaction. Cem Concr Res 36:395–400
9. BenHaha M, Gallucci E, Guidoum A, Scrivener KL (2007) Relation of expansion due to alkali silica reaction to the degree of reaction measured by SEM image analysis. Cem Concr Res 37:1206–1214
10. Giaccio G, Zerbino R, Ponce JM, Batic OR (2008) Mechanical behaviour of concretes damaged by alkali–silica reaction. Cem Concr Res 38:993–1004

11. Roma SN, Ngo T, Mendis P, Mahmud HB (2011) High-strength rice husk ash concrete incorporing quarry dust as a partial substituten for sand. Constr Build Mater 25:3123–3130
12. Okay O, Guclu H, Soner E (1985) Boron pollution in the Simav river, Turkey and various methods of boron removal. Water Res 19:857–862
13. Goldberg S (1997) Reactions of boron with soil. Plant Soil 193:35–48
14. Howe PD (1998) A review of boron effects in the environment. Biol Trace Elem Res 66:153–166
15. Boncukoglu R, Yılmaz TM, Kocakerim MM, Tosunoglu V (2002) Utilization of borogypsum as set retarder in Portland cement production. Cem Concr Res 32:471–475
16. Elbeyli İF, Derun EM, Gülen J, Pişkin S (2003) Thermal analysis of borogypsum and its effects on the physical properties of Portland cement. Cem Concr Res 33:1729–1735
17. Erdoğan Y, Genç H, Demirbaş A (1992) Utilization of borogysum for cement. Cem Concr Res 22:841–844
18. Erdoğan Y, Demirbaş A, Genç H (1994) Partly-refined chemical by-product gypsum as cement additives. Cem Concr Res 24:601–604
19. Kavas T, Olgun A, Erdoğan Y (2005) Setting and hardening of borogypsum-Portland cement clinker-fly ash blends. Studies on effects of molasses on properties of mortar containing borogypsum. Cem Concr Res 35:711–718
20. Demir D, Keleş G (2006) Radiation transmission of concrete including boron waste for 59.54 and 80.99 keV gamma rays. Nucl Instrum Methods Phys Res B 245:501–504
21. Demirbaş A, Karslıoğlu S (1995) The effect of boric acid sludges containing borogypsum on properties of cement. Cem Concr Res 25:1381–1384
22. Demirbaş A (1996) Optimizing the physical and technological properties of cement additives in concrete mixtures. Cem Concr Res 26:1737–1744
23. Demirbaş A (1999) Recyciling of lithium from borogypsum by leaching with water and leaching kinetics. Resour Conserv Recycl 25:125–131
24. Demirbaş A, Yüksek H, Çakmak İ, Küçük MM, Cengiz M, Alkan M (2000) Recovery of boric acid from boronic wastes by leaching with water, carbon dioxide- or sulfur dioxide-saturated water and leaching kinetics. Resour Conserv Recycl 28:135–146
25. Alp I, Deveci H, Süngün YH, Yazici EY, Savaş M, Demirci S (2009) Leachable characteristics of arsenical borogypsum wastes and their potential use in cement production. Environ Sci Technol 43:6939–6943
26. Tümen Y (2008) Effect of borogypsum on some properties of concrete. Masters thesis, Department of Civil Engineering, Mustafa Kemal University (in Turkish)
27. Sevim UK, Tümen Y (2013) Strength and fresh properties of borogypsum concrete. Constr Build Mater 48:342–347
28. Abell AB, Willis KL, Lange DA (1999) Mercury intrusion porosimetry and image analysis of cement-based materials. J Colloid Interface Sci 211:39–44
29. Khatib JM, Mangat PS (2003) Porosity of cement paste cured At 45 °C as a function of location relative to casting position. Cem Concr Res 25:97–108
30. Caré S (2008) Effect of temperature on porosity and on chloride diffusion in cement pastes. Constr Build Mater 22(7):1560–1573
31. Durmuş G, Arslan M (2010) Physical properties of cement mortars exposed to high temperature in various cooling conditions. J Fac Eng Arch Gazi Univ 25(3):541–548
32. ASTM D (1984) 4404: Standard test method for determination of pore volume and pore volume distribution of soil and rock by mercury intrusion porosimetry. ASTM International, Aug 31
33. ASTM C 1260–07 (2010) Standard test method for potential alkali reactivity of aggregates (Mortar-Bar method), American Society for Testing and Materials, West Conshohocken, Pennsylvania

34. Demir I (2010) The mechanical properties of alkali–silica reactive mortars containing same amounts of silica fume and fly ash. J Fac Eng Arch Gazi Univ 25(4):749–758
35. TS EN 196-1 (2002) Methods of testing cement—part 1: determination of strength. Turkish Standards, Ankara (in Turkey)
36. ASTM C 618 (2002) Standard specification for coal fly ash and raw or calcined natural pozzolan for use as a mineral admixture in Portland cement concrete. Annual book of ASTM standards, Pennsylvania
37. Bayca SU (2013) Microwave radiation leaching of colemanite in sulfuric acid solutions. Sep Purif Technol 105:24–32
38. Koçak Y, Taşcı E, Kaya U (2013) The effect of using natural zeolite on the properties and hydration characteristics of blended cements. Constr Build Mater 47:720–727
39. Gomes CEM, Ferreira OP, Fernandes MR (2005) Influence of vinyl acetate–versatic vinylester copolymer on the microstructural characteristics of cement pastes. Mater Res 8 (1):51–56
40. Govin A, Peschard A, Guyonnet R (2006) Modification of cement hydration at early ages by natural and heated wood. Cem Concr Compos 28(1):12–20
41. Cvetkovic J, Petrusevski VM, Soptrajanov B (1997) Reinvestigation of the water bending region in the spectra of gypsum-like compounds an FTIR study. J Mol Struct 408(409):463–466
42. Frost RL, Xi Y, Scholz R, Belotti FM, Filho MC (2013) Infrared and Raman spectroscopic characterization of the borate mineral colemanite—$CaB_3O_4(OH)_3{\cdot}H_2O$—implications for the molecular structure. J Mol Struct 1037:23–28